Silver nanoparticles enhanced photoluminescence of Nd^{3+} doped germanate glasses at 1064 nm

Luciana R.P. Kassab [a], Davinson M. Silva [a], José A.M. Garcia [b], Diego S. da Silva [b], Cid B. de Araújo [c, *]

[a] Laboratório de Tecnologia em Materiais Fotônicos e Optoeletrônicos, Faculdade de Tecnologia de São Paulo, CEETEPS/UNESP, 01124-060, São Paulo, SP, Brazil
[b] Departamento de Engenharia de Sistemas Eletrônicos, Escola Politécnica, Universidade de São Paulo, 05508-970, São Paulo, SP, Brazil
[c] Departamento de Física, Universidade Federal de Pernambuco, 50670-901, Recife, PE, Brazil

ABSTRACT

Infrared photoluminescence (PL) properties of PbO-GeO$_2$ glasses containing neodymium ions (Nd^{3+}) and silver nanoparticles (NPs) were investigated. The excitation was made with a continuous-wave diode laser operating at 805 nm, in resonance with the Nd^{3+} transition $^4I_{9/2} \rightarrow {}^4F_{5/2}$. Growth of ~160% in the PL intensity at 1064 nm, was observed in comparison with a reference sample without silver NPs. The PL enhancement is attributed to the increased local-field in the Nd^{3+} locations nearby the NPs. The present results indicate that PbO-GeO$_2$ glasses containing Nd^{3+} and silver NPs have good prospect to be used in optical amplifiers at 1064 nm.

© 2016 Elsevier B.V. All rights reserved.

1. Introduction

The presence of metallic nanoparticles (NPs) in glasses doped with rare-earth ions (REI) may enhance the glasses' photoluminescence (PL) properties due to: *i* - the enhanced optical field amplitudes in the vicinity of the NPs due to the mismatch between the dielectric function of the NPs and the host glass; *ii* - the absorption of light by the NPs followed by energy transfer to the REI; *iii* − the large growth of the optical field due to the excitation of localized surface plasmons (LSP) in the NPs [1–4].

The PL enhancement depends on the distance between the NPs and the REI, the volume fraction of the sample occupied by the NPs, the NPs size and shape, and the light wavelength (λ). The LSP resonance wavelength (λ_{SP}) depends on the size and shape of the NPs as well as on the host and the metal dielectric functions [1–4]. When $\lambda \approx \lambda_{SP}$, the PL enhancement due to the increased local-field, as well as the absorption of light by the NPs followed by energy transfer to the REI, may be very large. When λ is much different than λ_{SP}, the influence of the LSP and the enhanced absorption rate are not large and the most important contribution from the NPs is

due to the Purcell effect [1,3] for the emissions with wavelengths near to λ_{SP}.

Currently the search for glasses exhibiting large PL enhancement due to the incorporation of metallic NPs is a topical subject motivated by applications in devices, such as lasers, optical amplifiers, color displays, and solar cells.

For instance, silicates, borates, phosphates, antimony, as well as tellurium, bismuth and germanium oxides have been investigated by several authors [4–16]. In particular the glass composition 60PbO-40GeO$_2$ (in wt. %) − labeled as PGO − doped with REI and containing silver or gold NPs has been extensively investigated. PGO glasses present high refractive index (≈ 1.9), large transmittance from 400 to 4500 nm, low energy cutoff phonons (≈ 700 cm^{-1}), large chemical stability and high resistance to moisture. Enhanced optical properties were studied under various excitation conditions with samples singly-doped (Pr^{3+}, Er^{3+}, Eu^{3+}, Tm^{3+}, Tb^{3+}, Nd^{3+}), doubly-doped (Yb^{3+}/Er^{3+}, Yb^{3+}/Tm^{3+}, Tb^{3+}/Eu^{3+}), and triply-doped (Yb^{3+}/Tm^{3+}/Er^{3+}, Yb^{3+}/Tm^{3+}/Ho^{3+}) containing silver or gold NPs [16–26]. Pure and assisted-phonon electronic transitions [16–20] and white-light-generation [21,22] have been studied. Third-order nonlinearity studies of PGO (bulk samples and thin films), with and without metallic NPs, were reported and their possible applications as saturable absorbers or optical limiters in the visible range were demonstrated [23,24]. Also

it was shown that PGO thin films with gold NPs may be useful for all-optical switching in the infrared because their nonlinear refractive indices are larger by more than one order of magnitude than the values obtained for films without gold NPs [23]. In all cases it was observed that the metallic NPs contributed for enhancement of the optical properties and in some cases growth of one order of magnitude was obtained in the PL signals in the visible range. Recently PGO glass containing Nd^{3+} and silver NPs was exploited as infrared-to-visible frequency upconverter for excitation at 805 nm and the contribution of the NPs was characterized [26].

However, the influence of metallic NPs on the infrared emission of REI doped PGO glass was seldom studied [25]; RIB waveguides amplifiers were fabricated and gain enhancement at 1.53 μm, from 2 db/cm to 4.3 db/cm, was observed due to the influence of metallic NPs [25].

Although in the visible range individual silver NPs provide important contribution for PL enhancement due to λ_{SP} in the blue-green region, for PL in the infrared other contributions could be more important. For instance, NPs aggregates present red-shifted LSP resonance due to the NPs-NPs collective interactions [27], and may provide important contribution for PL growth in the infrared. Also energy transfer from NPs aggregates to the emitting ions can be very important as demonstrated in Refs. [28–30] for various physical systems.

The main motivation for the present work was to characterize the influence of silver NPs and their aggregates on the PL of Nd^{3+} doped PGO glasses in the near infrared (≈ 1.06 μm) aiming the evaluation of this material to develop efficient optical amplifiers. The samples studied were prepared with 100% more silver nitrate ($AgNO_3$) than in the previous experiments [26] in order to obtain larger PL enhancement at 1064 nm. The observed behavior was compared with the one described in Ref. [25] in order to identify the potential of the Nd^{3+} doped PGO glasses to be used as optical amplifier at 1064 μm.

2. Experimental details

Glassy samples with composition 60PbO-40GeO$_2$ (in wt. %) were obtained by the melting-quenching method with the addition of Nd_2O_3 (1.0 wt %) and $AgNO_3$ (2.0 wt %) to the original composition. The reagents were melted in an alumina crucible for 1 h at 1200 °C, quenched in air in a preheated brass mold, and annealed at 420 °C for 1 h to avoid internal stress. The samples were polished, cut, and then heat-treated for 24, 48 and 72 h to thermally reduce the Ag^+ ions to Ag^0 and nucleate silver NPs following the procedure reported in previous studies [16–23,26]. A sample without $AgNO_3$ was prepared to be used as reference. Also samples with Nd_2O_3 concentrations of 0.2 and 0.5 wt %, without silver NPs, were prepared to verify possible energy transfer processes involving Nd^{3+} ions contributing for the 1064 μm emission.

A 200 kV transmission electron microscope (TEM) was employed to investigate the presence of NPs in the samples and Energy Dispersive Spectroscopy (EDS) was used to verify the elements contained in the samples.

Linear absorption and PL were the techniques used to characterize the optical behavior of the samples. The absorption spectra were recorded from 400 to 1200 nm using a commercial spectrophotometer. The PL spectra were obtained exciting the samples with a continuous-wave diode laser operating at 805 nm, with the beam chopped at 70 Hz. The PL signals were collected in a direction perpendicular to the incident beam and analyzed by a monochromator equipped with a Ge photodetector with output fitted to a lock-in amplifier connected to a personal computer. Measurements of the PL intensity versus the Nd_2O_3 concentration and PL decay time were also performed. The samples were kept at room temperature during all measurements.

3. Results and conclusions

Fig. 1(a) shows TEM micrographs of the sample heat-treated for 48 h, obtained in a region of larger NPs concentration. Isolated NPs and aggregates of sub-micrometer dimensions are observed. Fig. 1(b) shows the histogram of sizes distribution of the isolated silver NPs presenting average size of 20 nm. The NPs growth occurs during the heat-treatment at 420 °C because at this temperature the material viscosity is enough to favor the Ag^+ diffusion. The formation of neutral silver atoms (Ag^0) is described by two types of reactions: $Ag^+ + Ag^+ \rightarrow Ag^{2+} + Ag^0$ and $Ag^+ + e^- \rightarrow Ag^0$. Afterwards, the Ostwald ripening and the NPs migration followed by coalescence originate formation of isolated NPs and aggregates. We observed that heat-treatment of the samples for long time intervals favor the formation of NPs aggregates and the formation of complex structures. The silver composition of the NPs was verified through EDS measurements with the results shown in Fig. 1(c).

Fig. 2 shows the absorption spectrum of a PGO: Nd^{3+} sample without silver NPs and the spectra of samples containing NPs, annealed at 420 °C for different time intervals. Absorption bands associated with Nd^{3+} transitions starting from the ground state, $^4I_{9/2}$, to the various excited states are shown. Absorption bands associated with the LSP resonances in individual NPs or aggregates are not observed. Due to the large refractive index of the PGO glass, the LSP absorption band of individual NPs should be in the range 420 nm–500 nm and it is expected to be broad because of the diverse sizes and shapes of the NPs. We recall that the LSP band was observed in PGO samples with large amount of metallic NPs [17,19]. Also the aggregates, expected to present LSP resonances red-shifted with respect to the isolated NPs, were not clearly observed in the present experiments. We attribute the absence of the resonance features to the small amount of $AgNO_3$ added to the glass starting composition. However it is observed in Fig. 2 a background from 400 nm to 1200 nm that is larger for the samples heat-treated for longer times, and the TEM images indicate clearly the presence of isolated NPs and aggregates. Also given in Fig. 2 are the absorption cross-sections corresponding to the Nd^{3+} transitions.

Fig. 3(a) shows a simplified energy levels diagram of Nd^{3+} and indicates the excitation ($^4I_{9/2} \rightarrow ^4F_{5/2}$) and the PL ($^4F_{3/2} \rightarrow ^4I_{11/2}$) transitions exploited in this work. The transition from the state $^4F_{5/2}$ to the state $^4F_{3/2}$ is nonradiative. Fig. 3(b) shows the PL spectrum corresponding to transition $^4F_{3/2} \rightarrow ^4I_{11/2}$, centered at 1064 nm, for the sample without silver NPs and for samples heat-treated during 1, 24, 48 and 72 h. Notice that the highest emission is observed for the sample annealed during 48 h and it corresponds to an enhancement of ~160% with respect to the sample without NPs; however the wavelengths of the incident light at 805 nm and the PL at 1064 nm are far from the λ_{SP} associated to the individual NPs. Notice that PL quenching occurs for the sample annealed during 72 h since long heat-treatment time intervals lead to large NPs concentration and aggregates formation. In such case the relative distances between Nd^{3+} and the NPs are reduced favoring energy transfer from the excited Nd^{3+} to the nearby NPs [1,4]. Notice also from Fig. 1(a) that most of the NPs nucleated in the present study are not as spherical as those presented in Ref. [26]. For nonspherical NPs the field enhancement is considerably larger than that for a comparable size spherical particle [1,3] due to the "lightning rod effect" and thus the nonspherical NPs and aggregates of irregular shapes contribute to obtain a large infrared PL enhancement. It is important to recall that the larger particles and the aggregates exhibit distinct dipole, quadrupole and even higher multipole resonances whose excitation produces local-fields external to the particles that may be larger than those produced by isolated NPs.
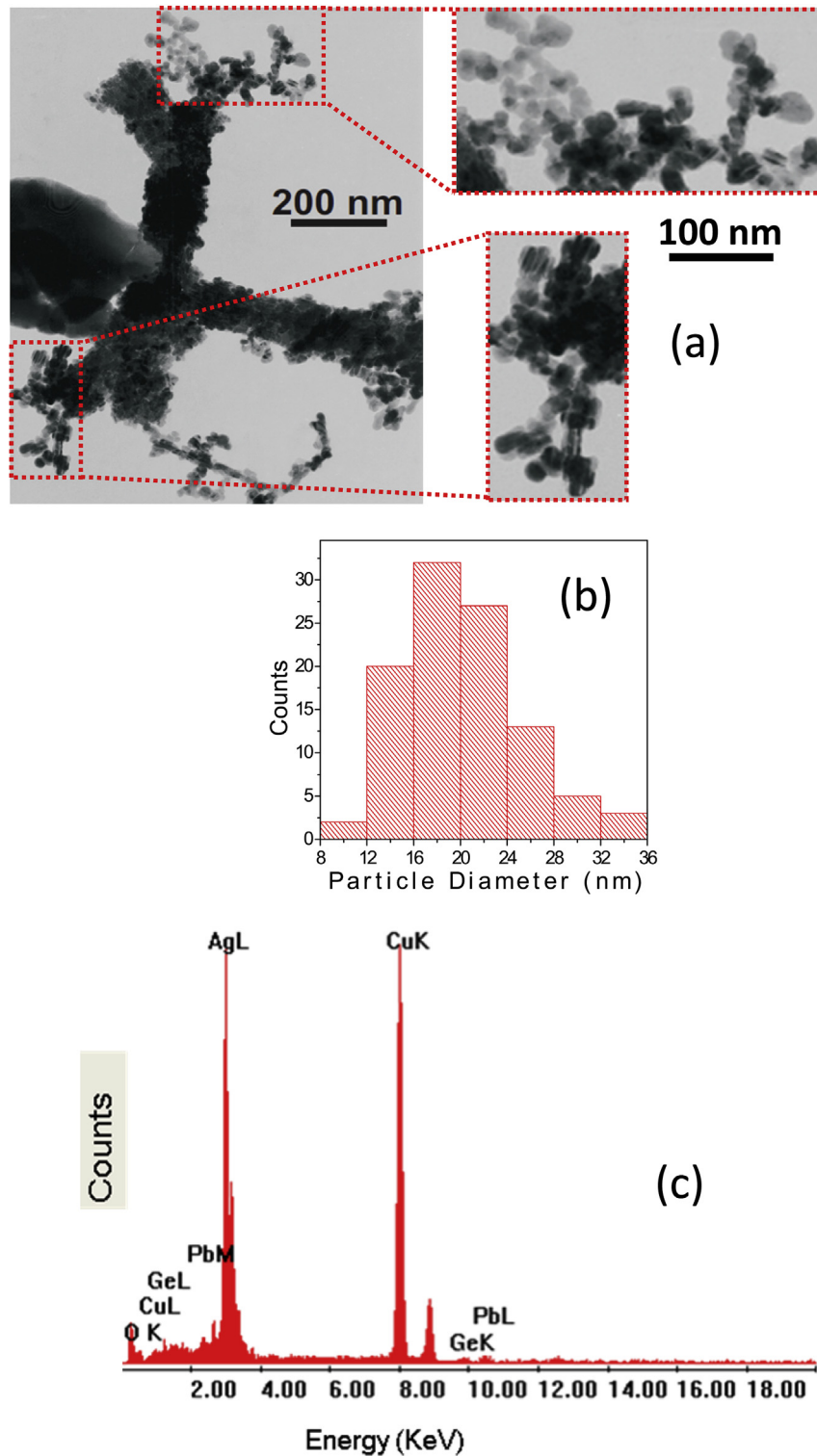
Fig. 1. TEM micrographs of the samples annealed for (a) 48 h; (b) average size distribution of the isolated nanoparticles; (c) EDS spectrum for a sample heat-treated during 48 h.

For example, Hao and Schatz [31] studying a silver NPs dimer of 36 nm, with separation of 2 nm between the particles, showed 3500-fold field enhancement due to a quadrupole resonance at 430 nm while the enhancement for a dipole resonance at 520 nm was one-order of magnitude only; the maximum electric field enhancement for both dipole and quadrupole resonances occur at the midpoint (hot-spot) between the two NPs. Therefore, the multipole resonances and the hot-spots contributions are very relevant to obtain the large PL enhancement at 1064 nm observed in the present experiments.

Measurements of the PL intensity at ≈1064 nm versus the laser intensity showed a linear behavior that indicates the participation of only one incident photon at 805 nm for each photon emitted at 1064 nm.
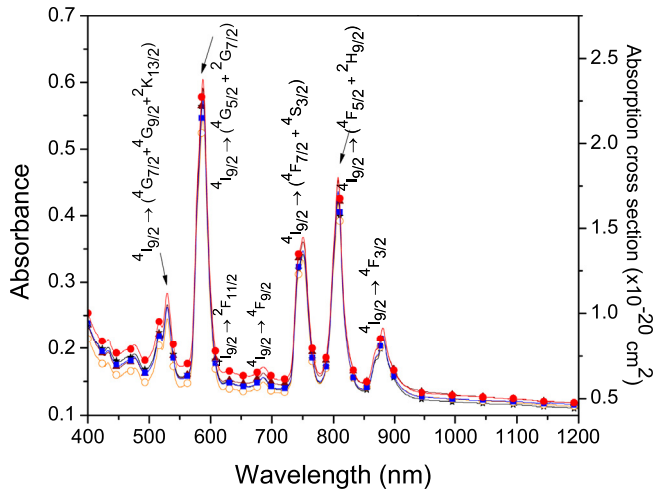
Fig. 2. Absorption spectra of Nd^{3+} doped PGO samples without NPs and containing NPs nucleated during different heat-treatment times: open circles (1 h), triangles (24 h), squares (48 h), full circles (72 h), stars (sample without silver NPs). Samples' thickness: 2 mm.
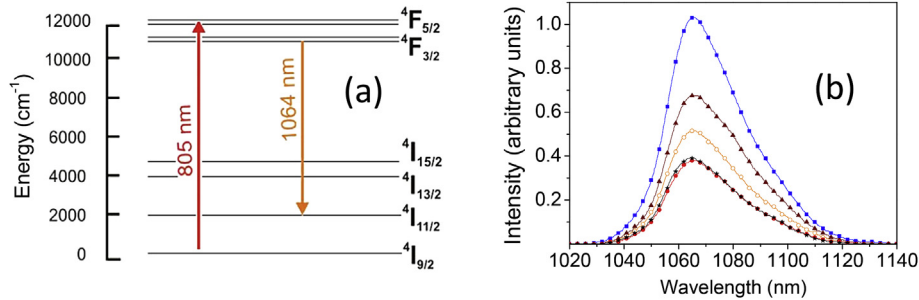
The quadratic dependence of the UC signals with the laser intensity and their linear dependence with the Nd^{3+} concentration were verified; however, the details are not given here because they were previously discussed in Ref. [26].

A log—log plot of the 1064 nm PL intensity as a function of Nd$_2$O$_3$ concentration is shown in Fig. 4. The slope of the straight line equal to 0.5 corresponds to a linear dependence of the signal amplitude with the Nd^{3+} concentration indicating that the PL at 1064 nm is due to the light absorption by single Nd^{3+}.

The characteristic time-decay, τ_d, of the 1064 nm signals was also measured and fitted by a single exponential. Decrease of τ_d in the presence of metallic NPs was observed in comparison with the samples without NPs. It was measured $\tau_d = 1.51 \pm 0.01$ ms for the sample heat-treated during 48 h, while for the reference sample we measured $\tau_d = 1.64 \pm 0.01$ ms. The reduction of τ_d is mainly due to the NPs influence. In other words, the decrease of τ_d is attributed to the increased density of photon modes in the vicinities of the NPs aggregates.

With basis on the present results it is not possible to assure that energy transfer from the aggregates is not contributing for the observed PL enhancement at 1064 nm. However, the decrease of τ_d

Fig. 3. (a) Simplified energy level scheme of Nd^{3+} with indication of the transitions studied. (b) Emission spectra of Nd^{3+} doped PGO samples, with and without silver NPs, heat-treated during different times: open circles (1 h), triangles (24 h), squares (48 h), full circles (72 h), stars (sample without silver NPs).

Infrared-to-visible frequency upconversion (UC) with emissions centered at 535 nm, 600 nm and 670 nm were also observed corresponding to the electronic transitions $^4G_{7/2} \rightarrow ^4I_{9/2}$, [$^4G_{7/2} \rightarrow ^4I_{11/2}$; $^4G_{5/2} \rightarrow ^4I_{9/2}$], and [$^4G_{7/2} \rightarrow ^4I_{13/2}$; $^4G_{5/2} \rightarrow ^4I_{11/2}$], respectively.
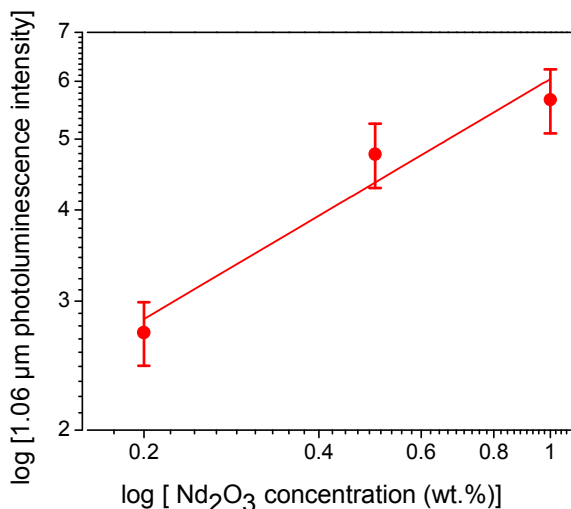
in the samples with metallic NPs indicates that the increased local-field acting on the Nd^{3+}, due to the hot-spots in the NPs aggregates, is providing the main contribution for the PL enhancement.

4. Summary

The results herein presented demonstrate the influence of the silver NPs on the infrared PL of Nd^{3+} doped PbO—GeO$_2$ glasses. The nucleation of silver NPs was obtained by conventional heat-treatment procedures. Maximum enhancement of $\approx$160% in the PL intensity at 1064 nm, obtained for the sample annealed for 48 h, is mainly attributed to the increased local-field produced by the NPs aggregates. The results indicate that Nd^{3+} doped PGO glasses with silver NPs present very good prospects as gain media for 1064 nm.

Fig. 4. Dependence of the PL intensity at 1064 nm versus the Nd$_2$O$_3$ concentration.

References

[1] P.N. Prasad, Nanophotonics, Wiley, New York, 2004.
[2] M. Yamane, Y. Asahara, Glasses for Photonics, Cambridge University Press, Cambridge, 2000.
[3] S.A. Meier, Plasmonics: Fundamentals and Applications, Springer, New York, 2007.
[4] Glass nanocomposites: synthesis, properties and applications, in: B. Karmakar, K. Rademann, A.L. Stepanov (Eds.), Micro & Nano Technologies Series, Elsevier, Cambridge, MA, 2016.
[5] O.L. Malta, P.A.S. Cruz, G.F. de Sá, F. Auzel, J. Lumin 33 (1985) 261–272.
[6] T. Som, B. Karmakar, J. Opt. Soc. Am. B 26 (2009) B21–B27.
[7] S.P.A. Osorio, V.A.G. Rivera, L.A.O. Nunes, E. Marega Jr., D. Manzani, Y. Messaddeq, Plasmonics 7 (2012) 53–58.
[8] D. Manzani, J.M.P. Almeida, M. Napoli, L. de Boni, M. Nalim, C.R.M. Afonso, S.J.L. Ribeiro, C.R. Mendonça, Plasmonics 8 (2013) 1667–1674.
[9] S. Fan, C. Yu, D. He, X. Wang, L. Hu, Opt. Mater. Express 2 (2012) 765–770.
[10] T.J. Antosiewicz, S.P. Apeli, Opt. Express 22 (2014) 2013–2042.
[11] A.L. Stepanov, Rev. Adv. Mater. Sci. 27 (2011) 115–145.
[12] M.H.A. Mhareb, S. Hashim, S.K. Ghoshal, Y.S.M. Alajerami, M.A. Saleh, R.S. Dawaud, N.A.B. Razak, S.A.B. Azizan, Opt. Mater 37 (2014) 391–397.
[13] Y.Y. Du, B.J. Chen, E.Y.B. Pun, Z.Q. Wang, X. Zhao, H. Lin, Opt. Commun. 334 (2014) 203–207.
[14] J.A. Jimenez, S. Sendova, C.Q. Zhao, Opt. Mater 46 (2015) 88–92.
[15] A. Herrera, S. Buchner, R.V. Camerini, C. Jacinto, N.M. Balzaretti, Opt. Mater 52 (2016) 230–236.
[16] C.B. de Araújo, L.R.P. Kassab, C.T. Dominguez, S.J.L. Ribeiro, A.S.L. Gomes, A.S. Reyna, J. Lumin 169 (2016) 492–496.
[17] C.B. de Araújo, L.R.P. Kassab, in: B. Karmakar, K. Rademann, A.L. Stepanov (Eds.), Glass Nanocomposites: Preparation, Properties, and Applications, Micro & Nano Technologies Series, vol. 5, Elsevier, Cambridge, MA, 2016, pp. 132–144.
[18] C.B. de Araújo, L.R.P. Kassab, R.A. Kobayashi, L.P. Naranjo, P.A.S. Cruz, J. Appl. Phys. 99 (2006) 123522.
[19] L.R.P. Kassab, D.S. da Silva, C.B. de Araújo, J. Appl. Phys. 107 (2010) 113506.
[20] M.S. Marques, L. de S. Menezes, W.B. Lozano, L.R.P. Kassab, C.B. de Araújo, J. Appl. Phys. 113 (2013) 053102.
[21] M.E. Camilo, T.A.A. Assumpção, D.M. da Silva, D.S. da Silva, L.R.P. Kassab, C.B. de Araújo, J. Appl. Phys. 113 (2013) 153507.
[22] M.E. Camilo, E. de O. Silva, L.R.P. Kassab, J.A.M. Garcia, C.B. de Araújo, J. Alloys Comp. 644 (2015) 155–158.
[23] C.B. de Araújo, T.R. Oliveira, E.L. Falcão-Filho, D.M. Silva, L.R.P. Kassab, J. Lumin 133 (2013) 180–183.
[24] L. De Boni, E.C. Barbano, T.A.A. de Assumpção, L. Misoguti, L.R.P. Kassab, S.C. Zilio, Opt. Express 20 (2012) 6844–6850.
[25] D.M. da Silva, L.R.P. Kassab, A.L. Siarkowski, C.B. de Araújo, Opt. Express 22 (2014) 16425–16430.
[26] D.S. da Silva, T.A.A. de Assumpção, L.R.P. Kassab, C.B. de Araújo, J. Alloys Comp. 586 (2014) S516–S519.
[27] J.Z. Zhang, C. Noguez, Plasmonics 3 (2008) 127–150.
[28] A. Chiasera, M. Ferrari, M. Matarelli, M. Montagna, S. Pelli, H. Portales, J. Zheng, G.C. Righini, Opt. Mater 27 (2005) 1743–1747.
[29] J.A. Jimenez, S. Lysenko, H. Liu, J. Appl. Phys. 104 (2008) 054313.
[30] M. Eichelbaum, K. Rademann, Adv. Funct. Mater 19 (2009) 2045–2052.
[31] E. Hao, G.C. Schatz, J. Chem. Phys. 120 (2003) 357–366.